In silico investigation of phytochemicals from *Entada rheedii* ethyl acetate leaf extract as potential inhibitors of the Bcl-xL protein

Nair Lekshmy R.[1], Duraipandian M.[2*] and Mini Gopinathan[2]
1. Department of Botany and Biotechnology, K.V.M. College of Arts and Science, Kokkothamangalam P.O., Cherthala, Alappuzha District 688527 Kerala, INDIA
2. Department of Biotechnology, Vivekanandha College of Arts and Sciences for Women (Autonomous), Elayampalayam, Tiruchengode, Namakkal District 637 205, Tamil Nadu, INDIA
*drduraipandian@vicas.org

Abstract

Colorectal cancer (CRC) is a major global health concern and remains the second leading cause of cancer-related mortality worldwide. A key hallmark of CRC progression is the evasion of apoptosis, often facilitated by the overexpression of anti-apoptotic proteins such as Bcl-xL. Inhibiting Bcl-xL is therefore a promising therapeutic strategy, but conventional inhibitors are limited by toxicity and reduced efficacy in Bcl-xL–overexpressing tumors. This study employed an in silico molecular docking approach to investigate phytochemicals from the ethyl acetate leaf extract of Entada rheedii as potential Bcl-xL inhibitors. The crystal structure of Bcl-xL (PDB ID: 2W3L) was retrieved from the Protein Data Bank, while the phytochemicals previously identified via LC–MS QTOF were obtained from the PubChem database. SwissADME was used to evaluate pharmacokinetic properties and AutoDock v1.5.7 was employed for docking simulations.

Docking results revealed that spiraeoside exhibited the strongest binding affinity (–7.8 kcal/mol), forming five hydrogen bonds and multiple hydrophobic interactions with active site residues of Bcl-xL. Although spiraeoside violated some drug-likeness rules due to its glycosylated structure, its binding strength and interaction profile identify it as a promising lead compound. Other flavonoids such as apigenin, genistein, luteolin and quercetin also demonstrated favorable pharmacokinetics and drug-like properties. This study highlights the potential of E. rheedii phytochemicals, particularly spiraeoside, as lead compounds for developing novel Bcl-xL inhibitors for colorectal cancer therapy. Further in vitro and in vivo validation is warranted to establish their biological efficacy and pharmacological feasibility.

Keywords: Colorectal cancer, Bcl-xL, *Entada rheedii*, Molecular docking, Phytochemicals, Spiraeoside.

Introduction

Colorectal cancer (CRC) is a significant global health concern and remains a leading cause of cancer-related mortality worldwide[7,20]. The development of CRC is a multi-step process, typically beginning with a benign adenomatous polyp that undergoes a series of successive genetic alterations to progress into an invasive adenocarcinoma[1]. A fundamental hallmark of this progression is the ability of malignant cells to evade apoptosis, or programmed cell death, which is a critical mechanism for eliminating damaged or abnormal cells[19]. This evasion contributes to both tumor progression and resistance to conventional therapies, highlighting the need for novel therapeutic strategies that can restore this cellular function[1,27].

The B-cell lymphoma 2 (Bcl-2) protein family plays a central role in regulating the intrinsic apoptotic pathway by maintaining a delicate balance between its pro-apoptotic and anti-apoptotic members[16]. In many cancers, this balance is skewed toward survival due to the overexpression of anti-apoptotic proteins like Bcl-xL[5,6]. Bcl-xL has emerged as a particularly attractive therapeutic target because its overexpression is strongly linked to tumor progression, invasiveness and resistance to chemotherapies such as fluorouracil (5-FU) [8]. While synthetic inhibitors of Bcl-xL show promise, they are often limited by on-target toxicities[7].

Phytochemicals, or naturally occurring compounds from plants, have garnered significant interest as a potential alternative class of therapeutic agents[14]. These compounds are often multi-targeted, providing a strategic advantage for overcoming the complex and redundant survival mechanisms of cancer cells. The phytochemicals present in the ethyl acetate leaf extract of *Entada rheedii* have been previously identified via LC–MS QTOF analysis, making it a promising source for screening against the Bcl-xL protein. This study aimed to identify and characterize novel lead compounds from these phytochemicals using an *in silico* molecular docking approach, a powerful computational technique for predicting molecular interactions and binding affinities.

Material and Methods

Target Selection: Data obtained from previous literature were used to obtain the most suitable protein target for colorectal cancer. The three-dimensional (3D) structures of the target protein Bcl-xL were obtained from the Protein Data Bank (PDB) database (*https://www.rcsb.org*) in PDB file format. The selected PDB ID for colorectal cancer target protein was 2W3L and was used for further study.

Target Preparation: The target protein was prepared by removing the complexed ligands using UCSF Chimera v.1.18[10] followed by energy minimization using the Minimize Structure tool.

Selection of Compounds: Compounds present in the ethyl acetate extract of *Entada rheedii* leaves identified previously using LC-MS QTOF were chosen as the ligands[11]. To conduct a comprehensive analysis of these compounds, their three-dimensional (3D) structures were obtained from the PubChem database (*https://pubchem.ncbi.nlm.nih.gov/*), a valuable repository for chemical information and structures. PubChem provides a diverse array of chemical compounds along with associated data.

Ligand Preparation: Absorption, distribution, metabolism and excretion (ADME) of ligand were performed using SWISS-ADME[4]. The SwissADME software was used to select compounds for molecular docking by evaluating their physicochemical properties, pharmacokinetics, water solubility, lipophilicity, medicinal chemistry and drug likeness (Lipinski's rule).

Molecular Docking and Visualization: The AutoDock v.1.5.7 was used to simulate the docking of the selected ligands against the target protein and the docking data with the highest binding score were displayed to examine the molecular interactions. The CASTp v.3.0 program was used to define and measure the volume and area of the active binding site of the target protein[21]. The amino acids which may participate in the docking in the active site were predicted and the affinity grid maps were identified using the AutoGrid tool of the AutoDock Tools package[8]. The weights and terms scoring function were set to default parameters. Furthermore, AutoDock uses a lamarckian genetic algorithm (LGA) for conformational searching and modes of ligands in the active receptor sites. AutoDock Vina, on the other hand, employs a gradient-optimization algorithm for conformational searching[22].

This method involves calculating the gradient of the potential energy function with respect to the ligand's degrees of freedom. The gradient information is then used to iteratively refine the ligand's conformation towards a local energy minimum. This approach is generally faster than the LGA used in AutoDock, making it suitable for large-scale virtual screening. Visualization was performed with the help of PyMOL v.3.1.1[18] and LigPlot+ v.2.2.9[6]. LigPlot represents the 2D representation of the docking interaction which include both H-bonds and hydrophobic interaction. H-bonds are represented in green dashed lines with donor-acceptor distance specified whereas red arcs represent hydrophobic interactions, with spokes spreading towards the ligand atoms. The 3D interactions are represented using PyMOL, where the cyan line represents the H-bond.

Ligand is represented as stick model in the 3D representation of H-bonding and the surface that would be traced out by the surfaces of waters in contact with the protein at all possible positions, is also shown. The protein structure has been represented as surface model and the ligand is colored as stick model for the docked pose for easy identification. When analyzing the interaction data, the docking result shows interaction with the amino acids in the active site mentioned in the CASTp server, indicating successful docking.

Results and Discussion

Target Protein Selection and Visualization: The anti-apoptotic protein Bcl-xL (PDB ID: 2W3L) was retrieved from the Protein Data Bank and visualized to assess its structural features relevant to colorectal cancer studies. The three-dimensional conformation of the protein is shown in figure 1.

In the sphere representation (Figure 1A), the overall globular structure of Bcl-xL is depicted. The ribbon representation (Figure 1B) highlights the different chains in distinct colours, with the bound ligand displayed in stick format at the active site region. For subsequent docking analyses, chain A of the protein was selected (Figure 1C) as it illustrates the ribbon representation of the chain with greater clarity. Water molecules present in the crystal structure are represented as red spheres. The structural visualization confirmed the suitability of the Bcl-xL protein (PDB: 2W3L) for use in docking and interaction studies, providing a reliable target for investigating its role in colorectal cancer.

Selection of Compounds: Bioactive compounds present in the ethyl acetate extract of *Entada rheedii* leaves, previously identified through LC–MS QTOF analysis, were selected as ligands for the present study. The 3D structures of these compounds were successfully retrieved from the PubChem database to enable molecular docking and interaction analysis. The list of selected ligands along with their PubChem compound IDs (CIDs) and molecular properties is provided in table 1. The corresponding 2D chemical structures of these ligands are presented in table 2, giving a clear overview of their structural diversity.

The inclusion of flavonoids (e.g. kaempferol, apigenin, genistein), glycosides (e.g. astragalin, spiraeoside, juglanin) and other phytochemicals highlights the chemical diversity of the *Entada rheedii* leaf extract and provides a strong basis for investigating their potential interactions with the selected protein target.

Ligand Preparation: The ADME profiling of eight phytochemicals from *Entada rheedii* ethyl acetate leaf extract was performed using SwissADME. The results revealed substantial variability in their physicochemical, pharmacokinetic and drug-likeness characteristics. Compounds such as apigenin, genistein, luteolin and quercetin demonstrated favourable pharmacokinetic features including high gastrointestinal (GI) absorption, absence of P-gp substrate properties and compliance with Lipinski's rule of five, indicating good oral bioavailability. All four

compounds also showed inhibitory potential against key CYP isoforms (CYP1A2, CYP2D6 and CYP3A4), suggesting possible drug–drug interactions. Their bioavailability scores (0.55) further highlighted their suitability as drug-like candidates.

In contrast, astragalin, juglanin and spiraeoside, the glycosylated derivatives, exhibited low GI absorption and high topological polar surface area (TPSA >150 Å²), violating multiple drug-likeness rules (Lipinski, Veber and Muegge). These features suggest limited passive membrane permeability and poor oral bioavailability (bioavailability score: 0.17 for astragalin and spiraeoside; 0.55 for juglanin). Additionally, spiraeoside was predicted as a P-gp substrate, which may further restrict intracellular accumulation.

Loliolide, a small monoterpenoid, displayed distinct properties with high GI absorption, blood–brain barrier (BBB) permeability and excellent aqueous solubility. However, it violated lead-likeness criteria due to its low molecular weight (< 250 Da), which may limit its optimization potential as a drug candidate.

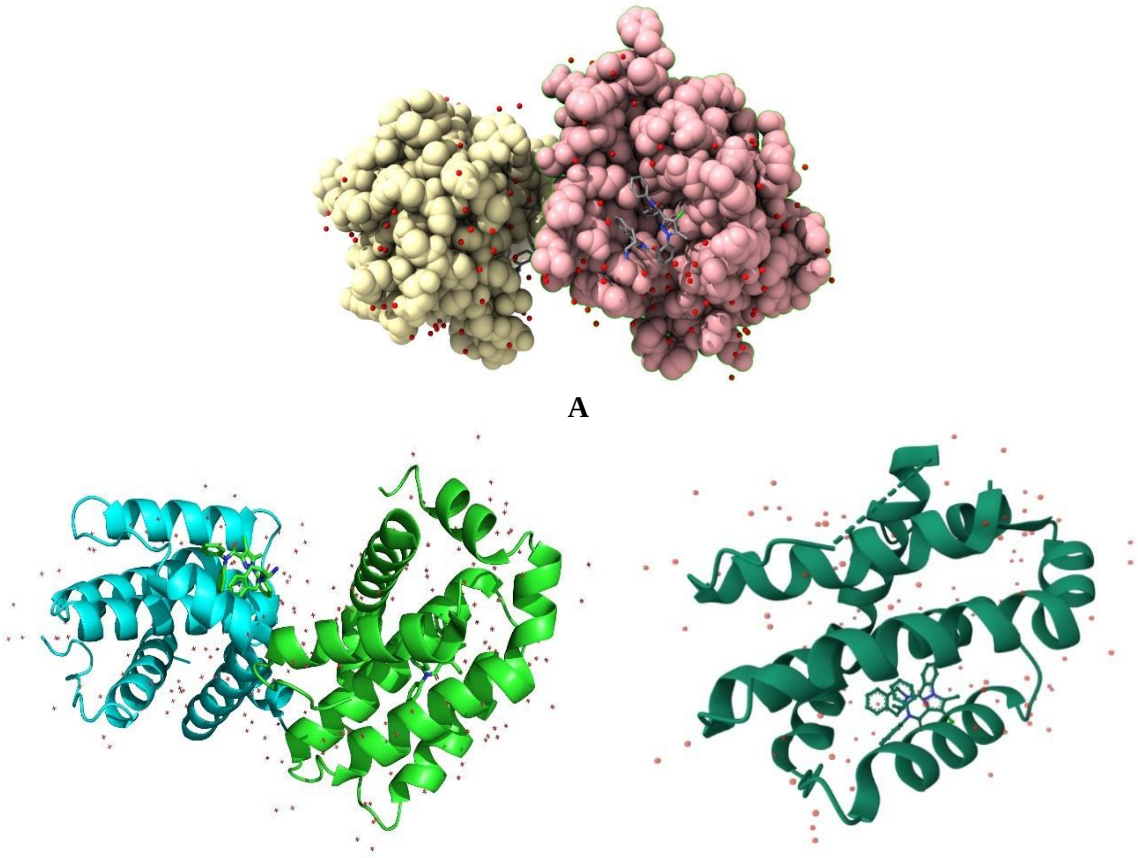

A

B **C**

Figure 1: The 3D structure of the target protein (PDB: 2W3L)
Figure A shows the sphere representation; B shows ribbon representation with chains labelled in different colours and ligand attached represented as stick model; and C showing ribbon model of the chain A of the target protein which was used for docking. Water molecules are represented as red dots

Table 1
Details of the ligands selected for analysis

S.N.	Name	Pubchem ID	Chemical Formula	Molecular Weight
1.	Apigenin	5280443	$C_{15}H_{10}O_5$	270.24 g/mol
2.	Astragalin	5282102	$C_{21}H_{20}O_{11}$	448.4 g/mol
3.	Genistein	5280961	$C_{15}H_{10}O_5$	270.24 g/mol
4.	Juglanin	5318717	$C_{20}H_{18}O_{10}$	418.3 g/mol
5.	Loliolide	100332	$C_{11}H_{16}O_3$	196.24 g/mol
6.	Luteolin	5280445	$C_{15}H_{10}O_6$	286.24 g/mol
7.	Quercetin	5280343	$C_{15}H_{10}O_7$	302.23 g/mol
8.	Spiraeoside	5320844	$C_{21}H_{20}O_{12}$	464.4 g/mol

Table 2
The 2D representation of ligands selected for analysis

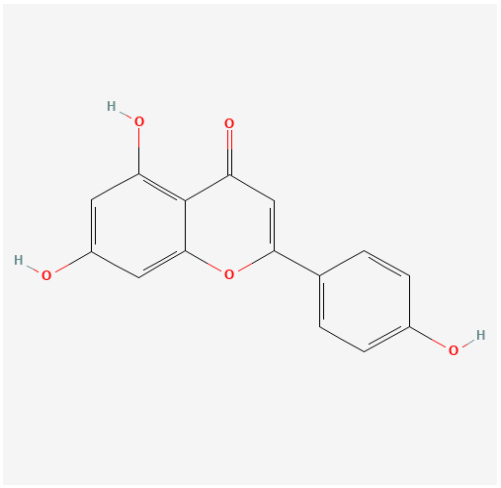	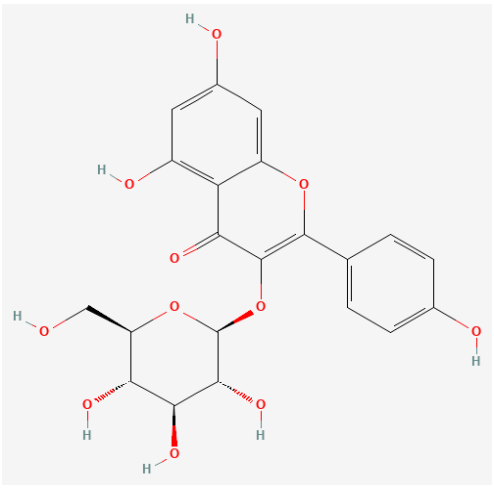
Apigenin	Astragalin
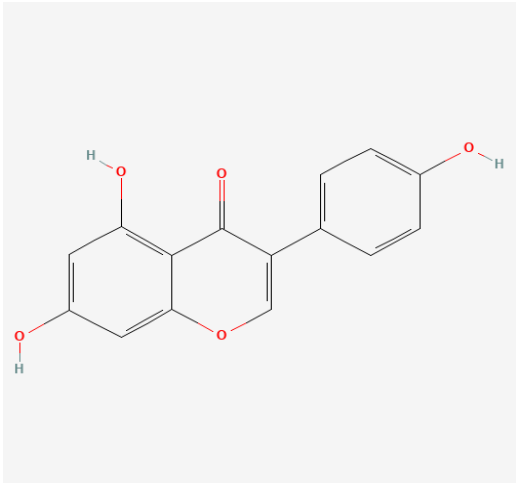	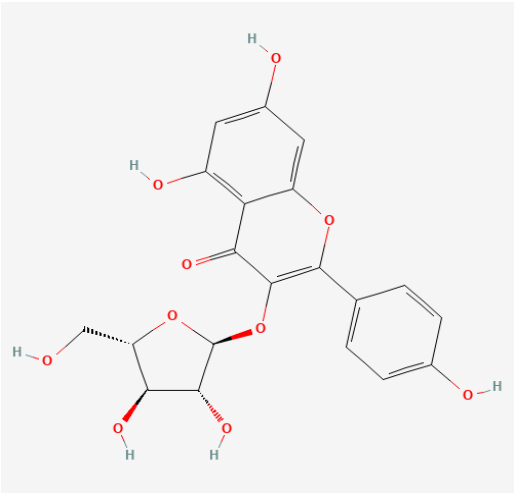
Genistein	Juglanin
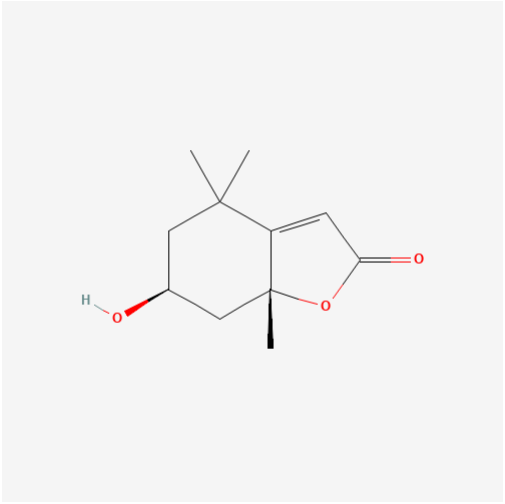	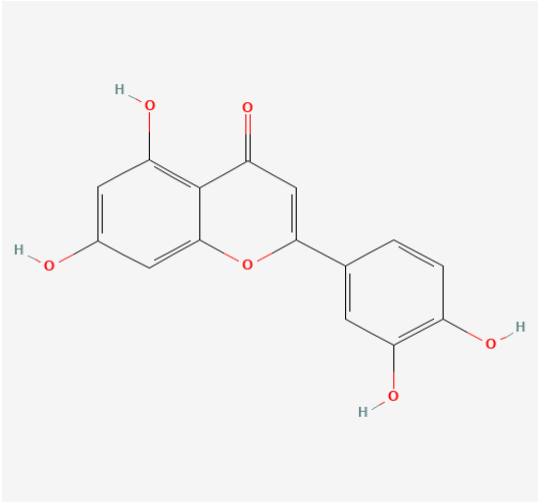
Loliolide	Luteolin

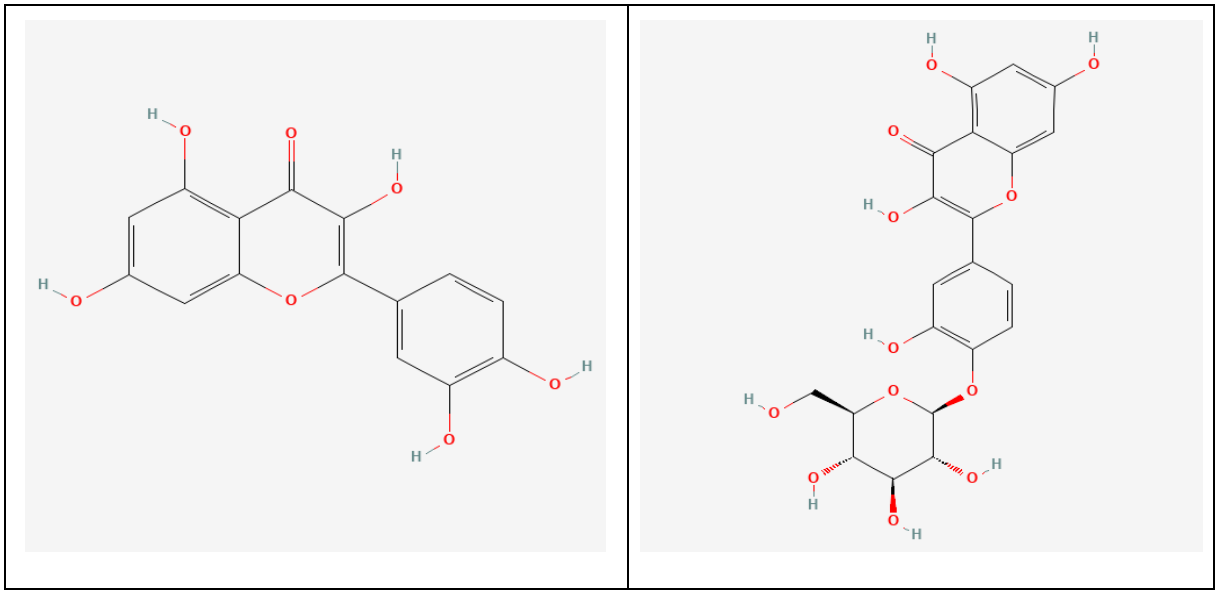

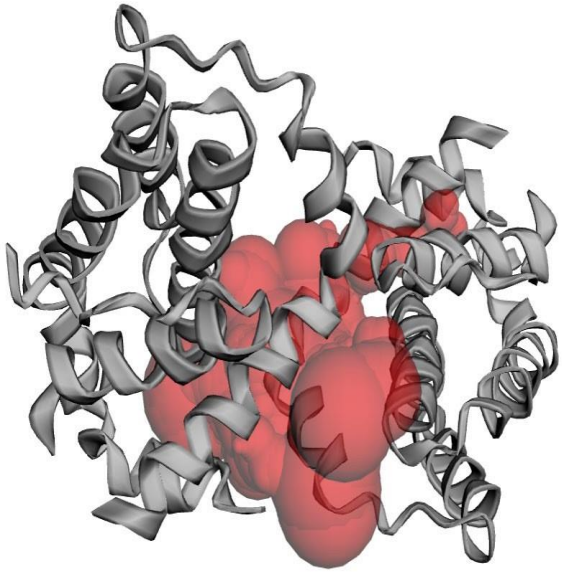

Figure 2: The binding chamber for the target protein 2W3L.
Fig. represents the binding chamber of the entire target protein

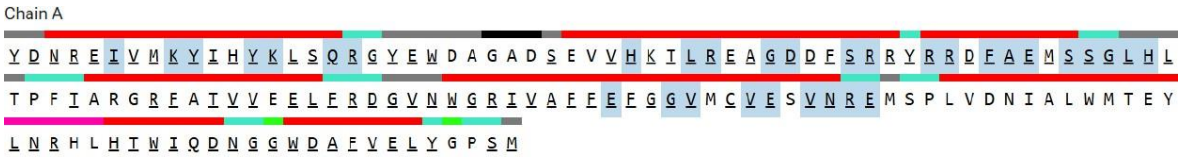

Figure 3: Amino acid sequence (single letter representation) of the 2W3L Chain A (target protein). Amino acids in the active site have been highlighted in blue colour

Regarding solubility, most flavonoids (apigenin, genistein, luteolin, quercetin) were categorized as soluble to moderately soluble, while astragalin, juglanin and spiraeoside showed variable solubility across different prediction models, likely influenced by their sugar moieties. Medicinal chemistry filters indicated no PAINS (pan-assay interference compounds) alert for most ligands, except for luteolin and quercetin, which showed catechol-related alerts.

Overall, apigenin, genistein, luteolin and quercetin emerged as promising drug-like phytochemicals with favorable oral pharmacokinetic properties. In contrast, glycosylated flavonoids such as astragalin, juglanin and spiraeoside, despite showing strong docking affinities, may face limitations in bioavailability. Loliolide, due to its small size and high BBB permeability, may represent a distinct scaffold with potential for CNS applications.

Molecular Docking Results

Active-site Prediction: CASTp was used to predict the docking site or active site for binding interaction. The area (Å 2) and volume (Å3) of active site for 2W3L were found

to be 1097.807 and 1344.234 respectively. The amino acids predicted by CASTp to participate in the docking are highlighted in figure 3. The binding chamber of the target protein is shown in figure 2.

Ligand–receptor docking affinity is represented by binding energy and interaction patterns. The optimal conformation of the ligand in the active pockets of the target depends on the magnitude of the negative binding affinity (lowest binding energy) used to evaluate docking output. Table 3 depicts the binding score which ranges from -7.8 to -5.9 kcal/mol with the corresponding bonding interaction. Thus, compound spiraeoside (-7.8 kcal/mol) showed the lowest binding affinity score. Upon interaction analysis, maximum number of hydrogen bonding (H-bonding) interaction was found for spiraeoside (5 hydrogen bonds) and maximum number of hydrophobic interactions was found for loliolide (8 hydrophobic interactions). The docking interactions and LigPlot representation are delineated in tables 4 –11.

Table 3
Affinity score, H- bonding of different ligands to target

Ligand Name	Binding Affinity (kcal/mol)	No. of H-Bonding	H-Bond forming Amino Acids	H-Bond Distance: Donor – Acceptor (Å)	Hydrophobic Interaction forming Amino Acids	No. of Amino Acids forming hydro-phobic bond
Apigenin	-6.9	1	Arg68(A)	2.99	Arg65(A) Asp61(A) Ser64(A) Val115(A) Arg26(A) Glu119(A) Val118(A)	7
Astragalin	-6.9	5	Gln252(A) Asp61(A) Ser75(A)	2.81 2.98 3.20 2.78 2.70	Lys22(A) Arg68(A) Arg26(A) Glu119(A) Val118(A) Val115(A) Gly114(A)	7
Genistein	-7.0	2	Arg86(A) His143(A)	2.95 2.90	Glu94(A) Phe89(A) Trp135(A) Ala90(A) Tyr139(A) Val93(A)	6
Juglanin	-7.4	3	Asn102(A) Ala59(A) Tyr161(A)	3.15 2.97 3.03	Leu160(A) Gly104(A) Arg105(A) Phe63(A) Asp62(A) Val107(A) Trp103(A)	7
Loliolide	-5.9	1	Ser75(A)	3.09	Ser64(A) Glu111(A) Phe71(A) Val115(A) Val118(A) Glu119(A) Lys22(A) Arg26(A)	8
Luteolin	-7.1	3	Arg68(A) Ser75(A)	2.97 2.92 2.83	Arg65(A) Ser64(A) Glu119(A) Val118(A) Arg26(A)	7

					Val115(A) Asp61(A)	
Quercetin	-7.1	3	Arg68(A) Ser64(A) Ser75(A)	3.33 2.91 2.82	Arg65(A) Asp61(A) Val115(A) Phe71(A)	4
Spiraeoside	-7.8	5	Arg86(A) Trp135(A) Glu138(A) Arg142(A) Ala90(A)	3.29 3.03 3.00 3.06 2.78	Phe89(A) Val93(A) Glu94(A) Phe97(A) Val101(A) His143(A) Tyr139(A)	7

Table 4
The visualization of docking interaction of Apigenin

<table>
<tr><td> 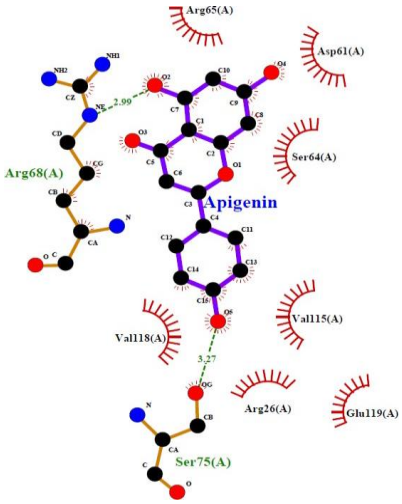
</td><td> 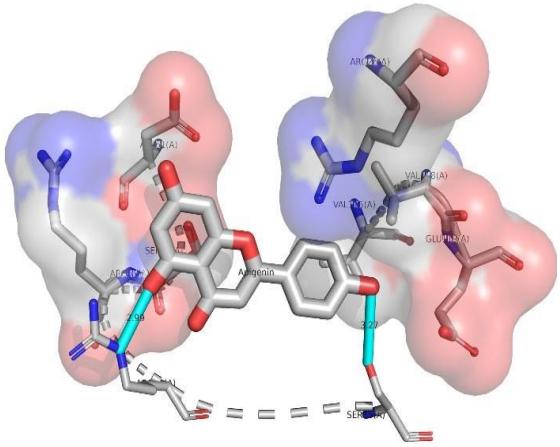 </td></tr>
<tr><td>2D representation of H-bonding of Apigenin with target</td><td>3D representation of H-bonding of Apigenin with target</td></tr>
<tr><td> 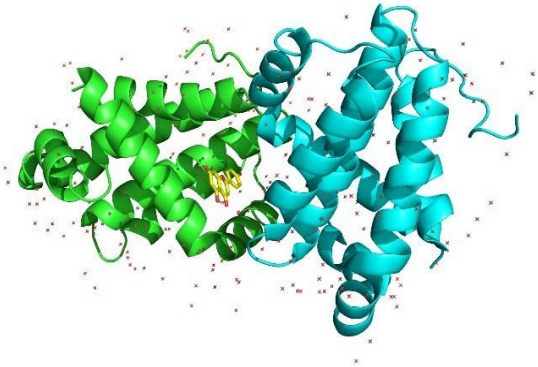 </td><td> 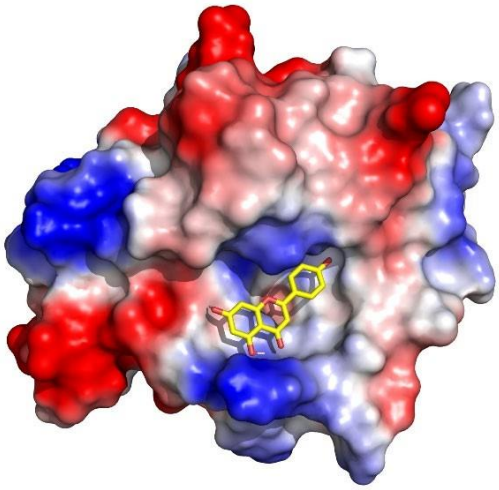 </td></tr>
<tr><td>3D representation of docked pose of Apigenin with target</td><td>3D representation of docked pose of Apigenin with target chain A</td></tr>
</table>

Table 5
The visualization of docking interaction of Astragalin

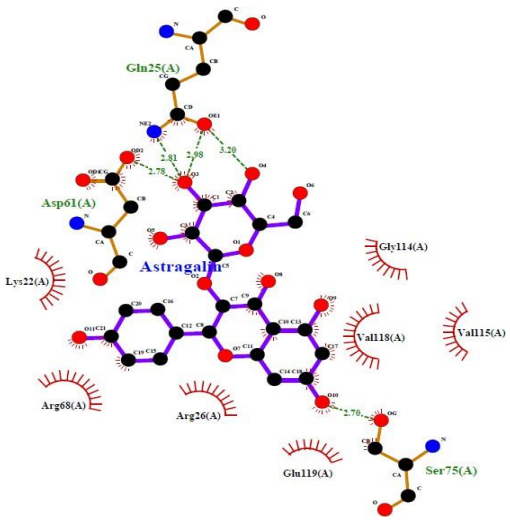	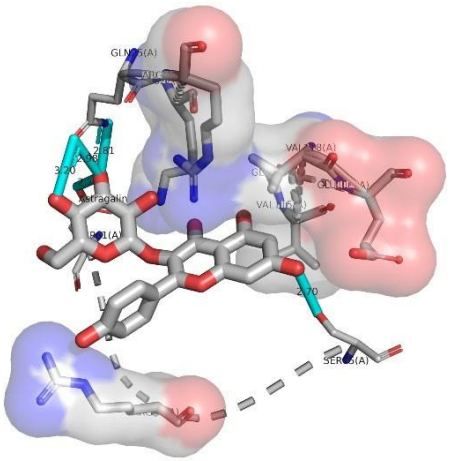
2D representation of H-bonding of Astragalin with target	*3D representation of H-bonding of Astragalin with target*
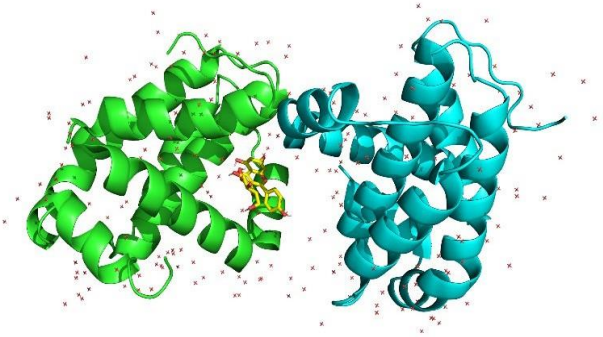	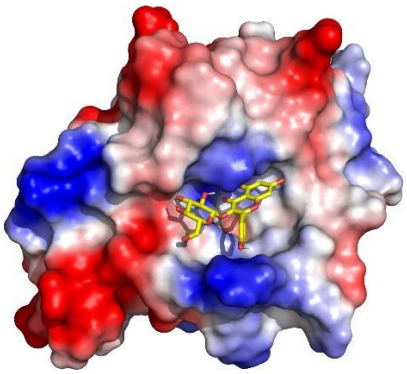
3D representation of docked pose of Astragalin with target	*3D representation of docked pose of Astragalin with target chain A*

Table 6
The visualization of docking interaction of Genistein

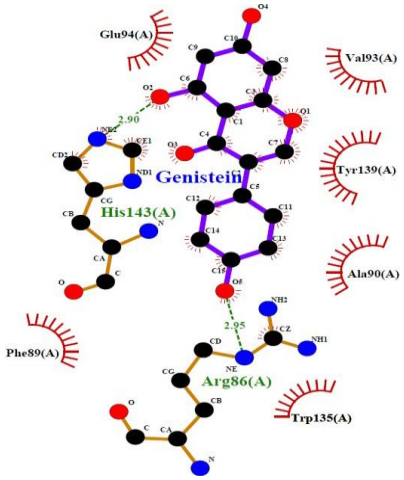	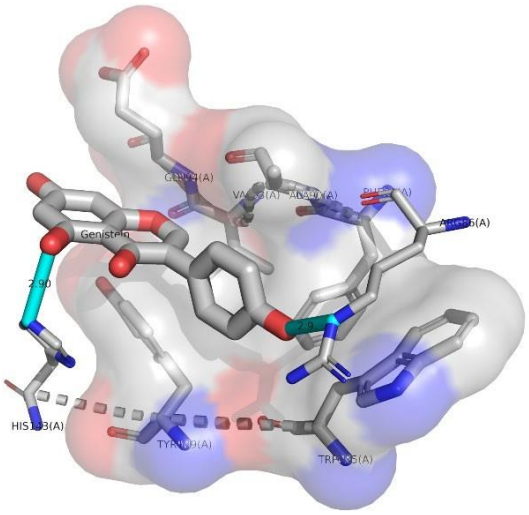
2D representation of H-bonding of Genistein with target	*3D representation of H-bonding of Genistein with target*

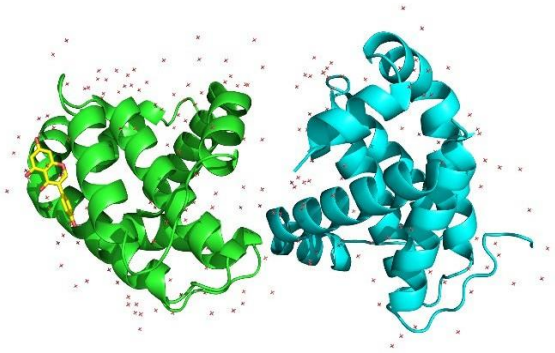	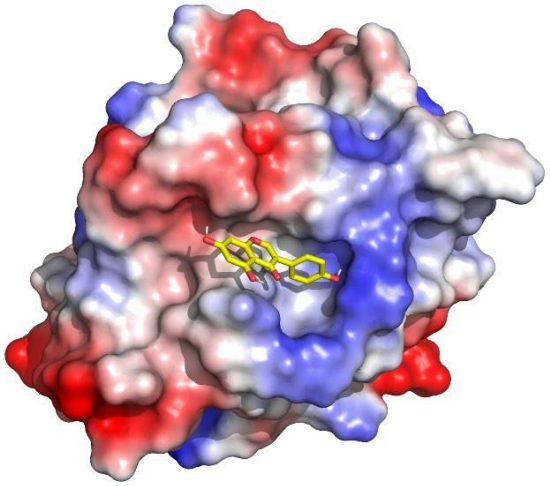
3D representation of docked pose of Genistein with target	*3D representation of docked pose of Genistein with target chain A*

Table 7
The visualisation of docking interaction of Juglanin

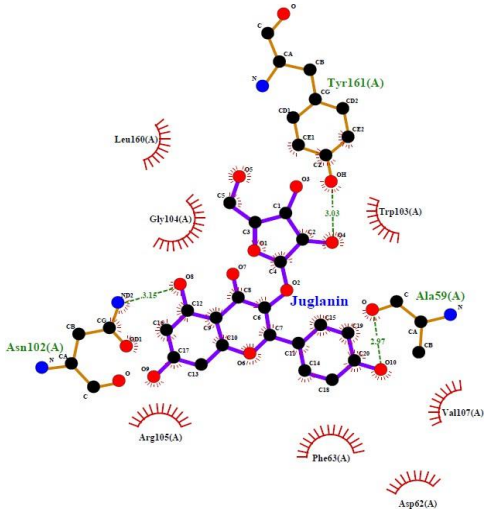	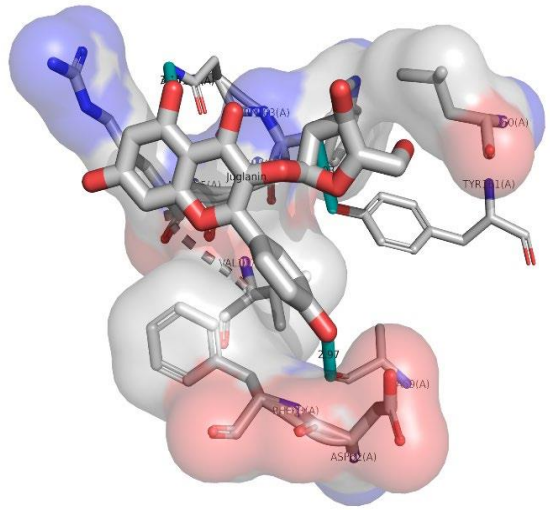
2D representation of H-bonding of Juglanin with target	*3D representation of H-bonding of Juglanin with target*
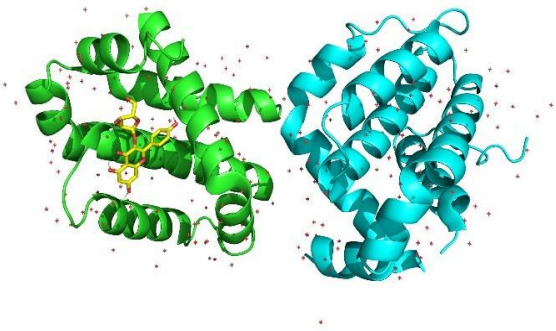	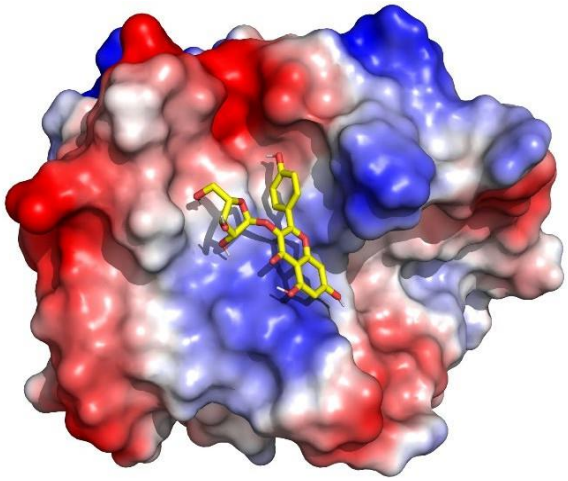
3D representation of docked pose of Juglanin with target	*3D representation of docked pose of Juglanin with target chain A*

Table 8
The visualization of docking interaction of Loliolide

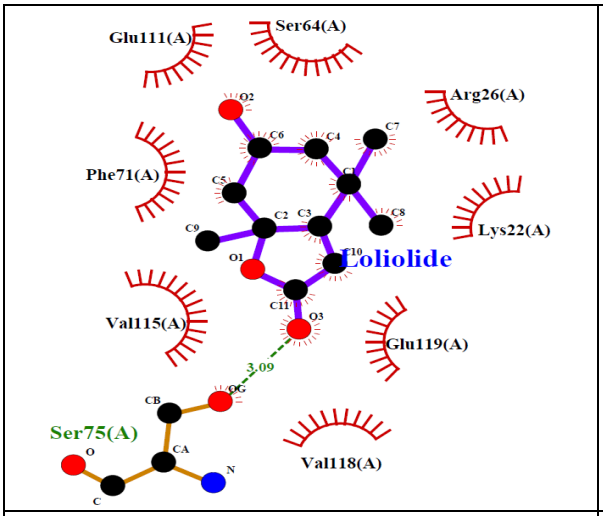	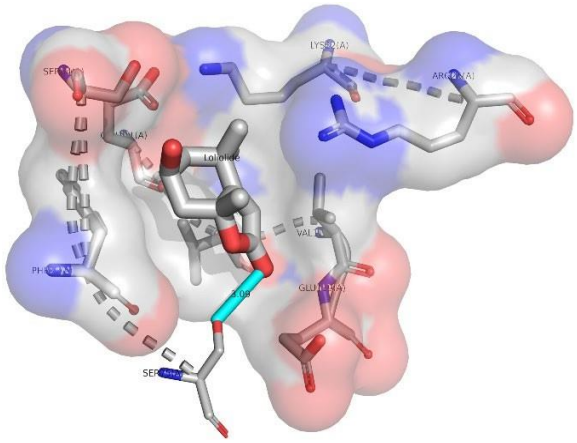
s2D representation of H-bonding of Loliolide with target	*3D representation of H-bonding of Loliolide with target*
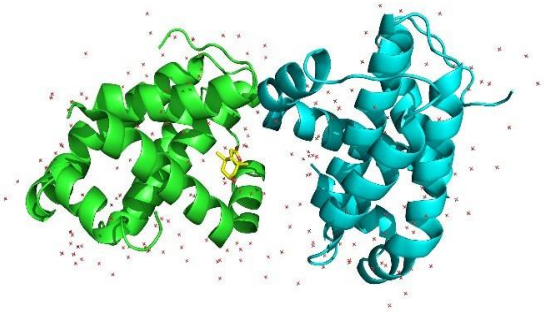	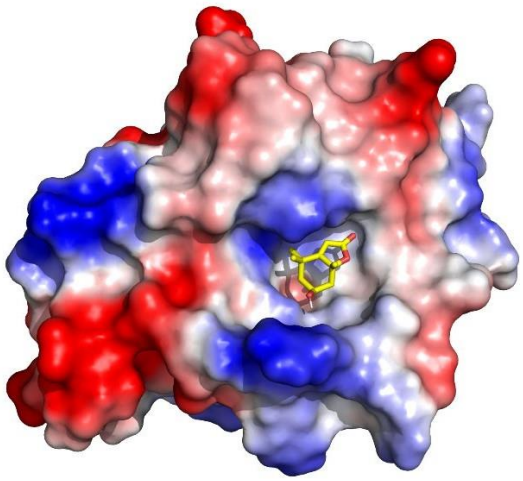
3D representation of docked pose of Loliolide with target	*3D representation of docked pose of Loliolide with target chain A*

Table 9
The visualization of docking interaction of Luteolin

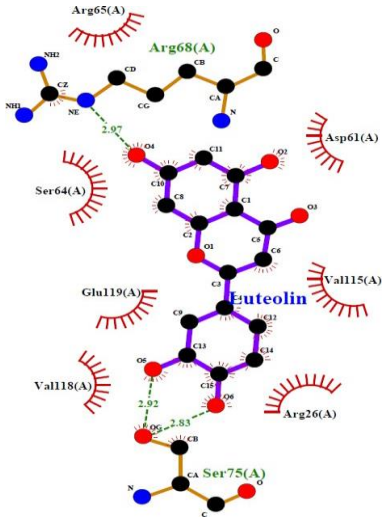	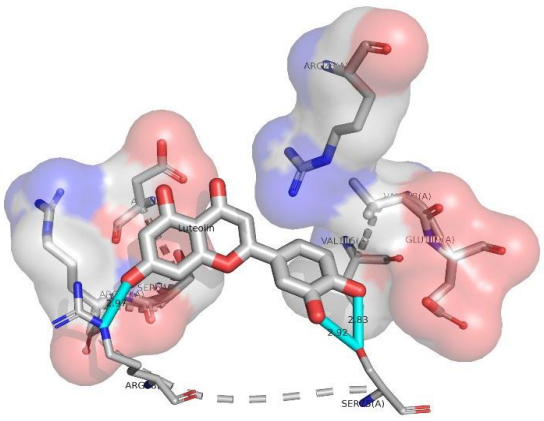
2D representation of H-bonding of Luteolin with target	*3D representation of H-bonding of Luteolin with target*

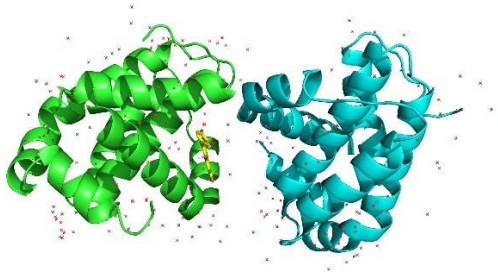	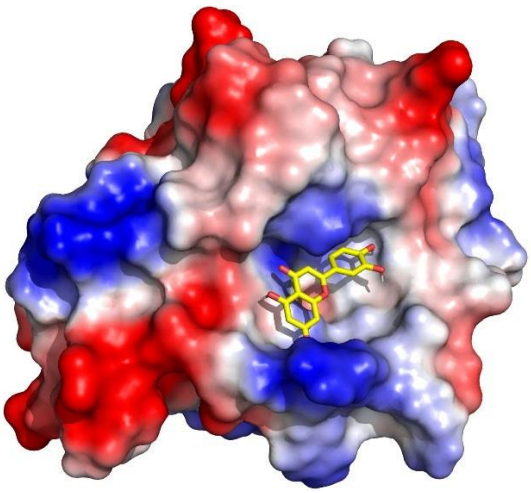
3D representation of docked pose of Luteolin with target	*3D representation of docked pose of Luteolin with target chain A*

Table 10
The visualization of docking interaction of Quercetin

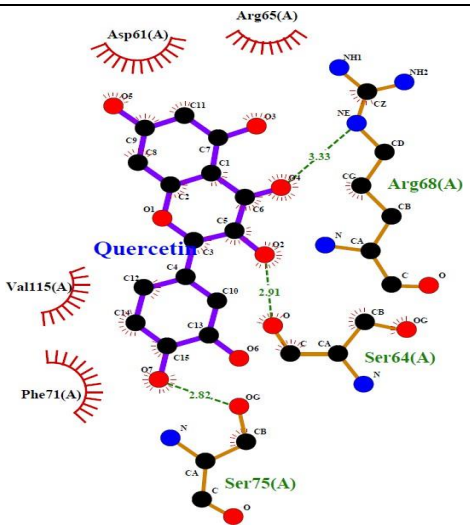	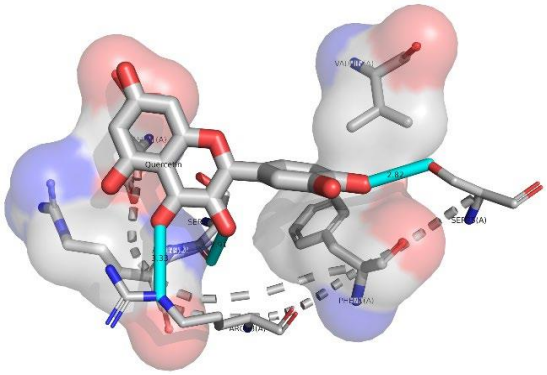
2D representation of H-bonding of Quercetin with target	*3D representation of H-bonding of Quercetin with target*
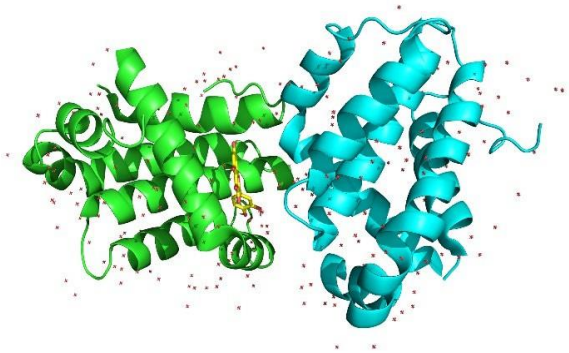	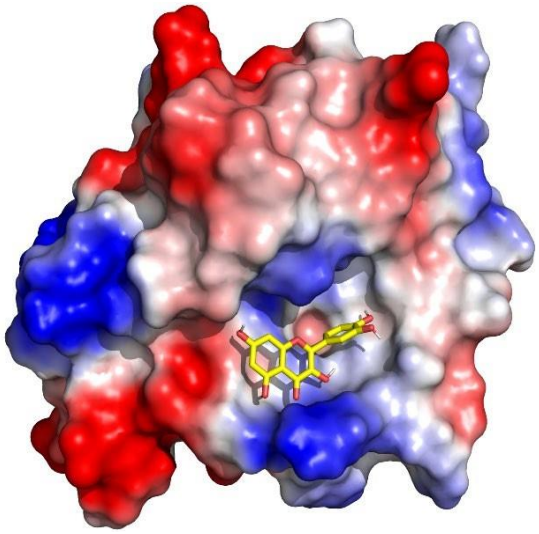
3D representation of docked pose of Quercetin with target	*3D representation of docked pose of Quercetin with target chain A*

Table 11
The visualization of docking interaction of Spiraeoside

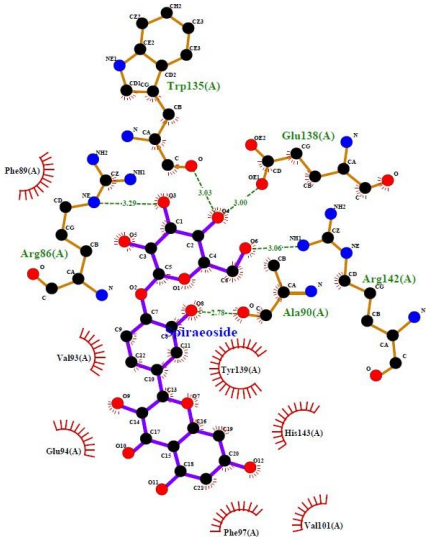	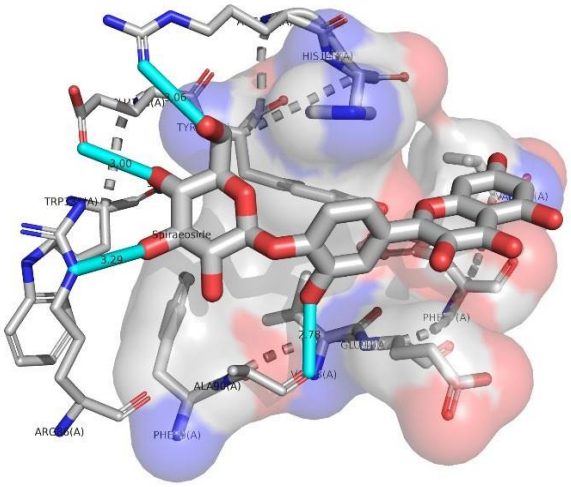
2D representation of H-bonding of Spiraeoside with target	*3D representation of H-bonding of Spiraeoside with target*
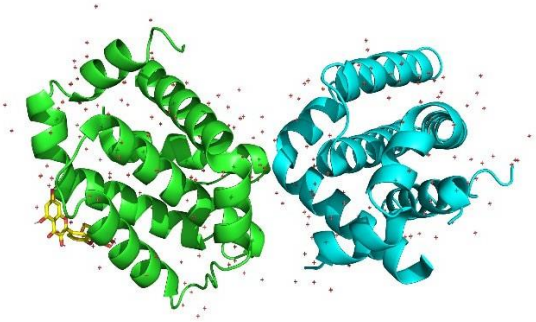	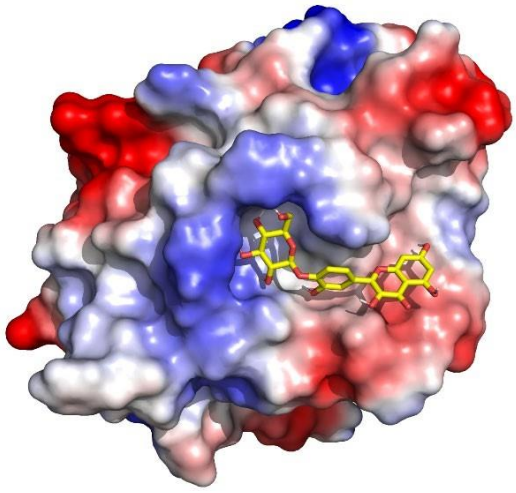
3D representation of docked pose of Spiraeoside with target	*3D representation of docked pose of Spiraeoside with target chain A*

The core objective of this study was to computationally screen phytochemicals from the ethyl acetate leaf extracts of *Entada rheedii* to identify potential inhibitors of the Bcl-xL protein, a critical anti-apoptotic target in colorectal cancer (CRC). Our molecular docking analysis successfully identified several compounds with binding potential, with spiraeoside emerging as the most promising candidate due to its high binding affinity (-7.8 kcal/mol) and favorable interaction profile with the Bcl-xL protein's active site. This finding is significant because it provides a new lead molecule for targeted therapy, offering a potential avenue to restore apoptosis in malignant cells that have become resistant to cell death signals. The results align with a growing body of research on the therapeutic potential of phytochemicals as anti-cancer agents. Natural compounds like curcumin, resveratrol and EGCG have been shown to exert anti-cancer effects by modulating various cellular pathways including the regulation of anti-apoptotic proteins like Bcl-xL[3],[13]. For example, in preclinical studies, curcumin has been shown to decrease the expression of Bcl-xL while increasing the levels of pro-apoptotic proteins, thereby inducing apoptosis[2]. Similarly, other phytochemicals have been found to bind directly to Bcl-2 family proteins, disrupting their pro-survival functions[22,26]. The finding that spiraeoside can bind to the Bcl-xL protein with a strong binding affinity, suggests it could act as a BH3 mimetic, a class of molecules designed to mimic pro-apoptotic proteins and inhibit the pro-survival activity of Bcl-xL.

This mechanism could be particularly effective in treating CRC, where Bcl-xL overexpression is a major driver of tumor progression and a source of resistance to therapies like fluorouracil (5-FU)[20]. While the high binding affinity of spiraeoside makes it a compelling lead compound, it is

important to consider other factors that influence a drug's efficacy and translational potential. The SwissADME analysis revealed that spiraeoside, a glycosylated flavonoid, violated several drug-likeness rules due to its high molecular weight and topological polar surface area (TPSA >150 Å²) which predict poor gastrointestinal absorption. This stands in contrast to other flavonoids in the extract such as Apigenin, Genistein, Luteolin and Quercetin, which demonstrated more favorable pharmacokinetic and drug-like properties.

These flavonoids, despite having lower binding affinities, are still valuable candidates for further investigation due to their better predicted oral bioavailability. Furthermore, the challenges associated with glycosidic compounds like spiraeoside could potentially be overcome through modern medicinal chemistry and drug delivery strategies. These include enzymatic or microbial deglycosylation within the gastrointestinal tract, which can release a more permeable and active aglycone locally at the colon[23], or the use of targeted delivery systems like pH-sensitive coatings or nanoparticles to improve absorption and efficacy[16]. Therefore, the promising results of this computational screening serve as a crucial first step, providing a clear roadmap for future research.

The next logical phase would be to conduct comprehensive *in vitro* studies to validate the findings. This would involve treating colorectal cancer cell lines with spiraeoside to confirm that it indeed induces apoptosis, modulates the expression of Bcl-xL and demonstrates a cytotoxic effect. If successful, subsequent *in vivo* studies using animal models would be essential to evaluate the compound's systemic efficacy, pharmacokinetics and safety profile[3]. Additionally, given the complexity of cancer and the potential for resistance, exploring combination therapies would be a critical direction. Future research could investigate the synergistic potential of spiraeoside with conventional chemotherapeutic agents like 5-FU, or with other targeted inhibitors, as demonstrated by other studies combining Bcl-xL inhibitors with MCL-1 inhibitors or with agents that modulate the Wnt pathway.

In conclusion, our *in silico* investigation has successfully identified spiraeoside from *Entada rheedii* as a lead compound with a strong potential to inhibit the anti-apoptotic Bcl-xL protein. This finding opens a new and exciting avenue for developing a phytochemical-based therapy for colorectal cancer. However, the true clinical relevance of these findings can only be determined through rigorous, multi-stage preclinical and clinical development, beginning with direct biological validation.

Conclusion

The present study concludes that spiraeoside shows a greater binding affinity for the human Bcl-xL protein (2W3L) based on protein-ligand interactions and binding energy values derived from molecular docking. The ligand with higher affinity has the potential to inhibit the activity of 2W3L which may lead to the suppression of its anti-apoptotic activity.

Acknowledgement

The authors gratefully acknowledge the facilities provided by Department of Botany and Biotechnology, KVM College of Arts and Science, Cherthala, Kerala and the Department of Biotechnology (DBT-FIST Sponsored Department) at Vivekanandha College of Arts and Sciences for Women (Autonomous), Elayampalam, Tiruchengode, Tamil Nadu, for carrying out this work.

References

1. Abraha A.M. and Ketema E.B., Apoptotic pathways as a therapeutic target for colorectal cancer treatment, *World J. Gastrointest. Oncol.*, **8**, 583 **(2016)**

2. Anto R.J., Mukhopadhyay A., Denning K. and Aggarwal B.B., Curcumin (diferuloylmethane) induces apoptosis through activation of caspase-8, BID cleavage and cytochrome c release: its suppression by ectopic expression of Bcl-2 and Bcl-xl, *Carcinogenesis*, **23**, 143–150 **(2002)**

3. Bandaru S.S., Tserenpil G., Veeraballi S., Rayad M.N., Merchant N., Boyilla R. and Nagaraju G.P., The Role of Phytochemicals in the Treatment of Colorectal Cancer, *Forum Immunopathol. Dis. Ther.*, **9**, 35–50 **(2022)**

4. Daina A., Michielin O. and Zoete V., SwissADME: a free web tool to evaluate pharmacokinetics, drug-likeness and medicinal chemistry friendliness of small molecules, *Sci. Rep.*, **7**, 42717 **(2017)**

5. Dakkak B.E., Taneera J., El-Huneidi W., Abu-Gharbieh E., Hamoudi R., Semreen M.H., Soares N.C., Abu-Rish E.Y., Alkawareek M.Y., Alkilany A.M. and Bustanji Y., Unlocking the therapeutic potential of BCL-2 associated protein family: exploring BCL-2 inhibitors in cancer therapy, *Biomol. Ther. (Seoul)*, **32**, 267–280 **(2024)**

6. Hafezi S. and Rahmani M., Targeting BCL-2 in Cancer: Advances, Challenges and Perspectives, *Cancers (Basel)*, **13**, 1292 **(2021)**

7. Hennessy E.J., Selective inhibitors of Bcl-2 and Bcl-xL: Balancing antitumor activity with on-target toxicity, *Bioorg. Med. Chem. Lett.*, **26**, 2105 **(2016)**

8. Judd A.S., Bawa B., Buck W.R., Tao Z.F., Li Y., Mitten M.J., Bruncko M., Catron N., Doherty G., Durbin K.R., Enright B., Frey R., Haasch D., Haman S., Haight A.R., Henriques T.A., Holms J., Izeradjene K., Judge R.A., Jenkins G.J., Kunzer A., Leverson J.D., Martin R.L., Mitra D., Mittelstadt S., Nelson L., Nimmer P., Palma J., Peterson R., Phillips D.C., Ralston S.L., Rosenberg S.H., Shen X., Song X., Vaidya K.S., Wang X., Wang J., Xiao Y., Zhang H., Zhang X., Blomme E.A., Boghaert E.R., Kalvass J.C., Phillips A. and Souers A.J., BCL-XL-targeting antibody-drug conjugates are active in preclinical models and mitigate on-mechanism toxicity of small-molecule inhibitors, *Sci. Adv.*, **10**, eado7120 **(2024)**

9. Laskowski R.A. and Swindells M.B., LigPlot+: multiple ligand-protein interaction diagrams for drug discovery, *J. Comput. Aided Mol. Des.*, **26**, 651–661 **(2011)**

10. Menon G. and Cagir B., Colon Cancer, StatPearls [Internet] **(2025)**

11. Morris G.M., Huey R., Lindstrom W., Sanner M.F., Belew R.K., Goodsell D.S. and Olson A.J., AutoDock4 and AutoDockTools4: Automated docking with selective receptor flexibility, *J. Comput. Chem.*, **30**, 2785–2791 **(2009)**

12. Nair L.R., Duraipandian M. and Gopinathan M., Characterization of ethyl acetate-based leaf extract of *Entada rheedii* Spreng. by using liquid chromatography quadrupole time-of-flight mass spectrometry, *Appl. Biol. Res.*, **27**, 271–284 **(2025)**

13. Paul J.K., Azmal M., Haque A.S.N.B., Talukder O.F., Meem M. and Ghosh A., Phytochemical-mediated modulation of signaling pathways: A promising avenue for drug discovery, *Adv. Redox Res.*, **13**, 100113 **(2024)**

14. Pawase P.A. et al, A conceptual review on classification, extraction, bioactive potential and role of phytochemicals in human health, *Future Foods*, **9**, 100313 **(2024)**

15. Pettersen E.F., Goddard T.D., Huang C.C., Couch G.S., Greenblatt D.M., Meng E.C. and Ferrin T.E., UCSF Chimera – a visualization system for exploratory research and analysis, *J. Comput. Chem.*, **25**, 1605–1612 **(2004)**

16. Piyush S., Satbhai B., Shah M. and Katti S., The evolution of prodrug strategies: From simple carriers to smart, targeted systems, *Int. J. Pharm. Sci.*, **3**, 4659–4574 **(2025)**

17. Qian S., Wei Z., Yang W., Huang J., Yang Y. and Wang J., The role of BCL-2 family proteins in regulating apoptosis and cancer therapy, *Front. Oncol.*, **12**, 985363 **(2022)**

18. Ramesh P. and Medema J.P., BCL-2 family deregulation in colorectal cancer: potential for BH3 mimetics in therapy, *Apoptosis*, **25**, 305–320 **(2020)**

19. Rao C.N.R., Chemical Applications of IR Spectroscopy, Academic Press, 250 **(1963)**

20. Scherr L., Gdynia G., Salou M., Radhakrishnan P., Duglova K., Heller A., Keim S., Kautz N., Jassowicz A., Elssner C., He W., Jaeger D., Heikenwalder M., Schneider M., Weber A., Roth W., Schulze-Bergkamen H. and Koehler B.C., Bcl-xL is an oncogenic driver in colorectal cancer, *Cell Death Dis.*, **7**, e2342 **(2016)**

21. Shahdeo Prakriti and Kumar Anil, Study of symptoms, cultural characteristic and isolation of Cercospora species causing tikka disease of ground in Ranchi district of Jharkhand, *Res. J. Chem. Environ.*, **29(2)**, 55-61 **(2020)**

22. Singh S., Bani Baker Q. and Singh D.B., Molecular docking and molecular dynamics simulation, Bioinformatics, Academic Press, 291-304 **(2021)**

23. Sordon S., Popłoński J. and Huszcza E., Microbial glycosylation of flavonoids, *Pol. J. Microbiol.*, **65**, 137–151 **(2016)**

24. Tian W., Chen C., Lei X., Zhao J. and Liang J., CASTp3.0: computed atlas of surface topography of proteins, *Nucleic Acids Res.*, **46**, W363–W367 **(2018)**

25. Trott O. and Olson A.J., AutoDock Vina: improving the speed and accuracy of docking with a new scoring function, efficient optimization and multithreading, *J. Comput. Chem.*, **31**, 455–461 **(2010)**

26. Verma S., Singh A., Kumari A., Tyagi C., Goyal S., Jamal S. and Grover A., Natural polyphenolic inhibitors against the antiapoptotic BCL-2, *J. Recept. Signal Transduct. Res.*, **37**, 391–400 **(2017)**

27. Zhang L., Pang Q., Wu Y., Wang Y., Wang Q. and Fan Y., Significance of Bcl-xL in human colon carcinoma, *World J. Gastroenterol.*, **14**, 3069 **(2008)**.

(Received 20th September 2025, accepted 18th October 2025)